University of Baghdad
College of Engineering
JE
JOURNAL OF ENGINEERING

Journal of Engineering

journal homepage: www.jcoeng.edu.iq

Volume 32 Number 11 November 2026



A Hybrid Enhancement Framework for Chest X-Ray Images Using CLAHE, Haar Wavelet, and Denoising Filters: A Quality Metrics Analysis

Mohanad Azeez Joodi *, Jaafar Ahmed Abdulsaheb

Department of Electrical Engineering, College of Engineering, University of Baghdad, Baghdad, Iraq

ABSTRACT

Chest radiographic imaging is one of the more frequently used diagnostic techniques in the diagnostic investigation of diseases. This study suggests a hybrid image enhancement technique that combines the contrast-limited adaptive Histogram Equalization (CLAHE) with Haar wavelet transformation, along without and with different noise-removing filters to enhance the chest X-ray images. To achieve better local contrast while preserving edges, the framework involves an adaptive clip limit in the CLAHE algorithm and an adaptive K-factor that is used to enhance Haar waveform detail. Besides, bilateral noise reduction, Wiener, nonlocal mean (NLM) filters, and cascade noise filters were explored to remove the image noise while maintaining the significant structural information. Typical chest X-ray images, both in normal and pneumonia conditions, were used to evaluate the proposed enhancement methods. Objective measures such as peak signal-to-noise ratio (PSNR), structural similarity index (SSIM), entropy, contrast, sharpness, and noise contrast have been used to quantify the image quality. Experimental results indicate that adaptive modification of the CLAHE clip limit and Haar wave K index greatly enhances the quality of images in comparison to conventional enhancement. Moreover, applying the right filters for noise reduction can preserve the structure and reduce noise amplification without sacrificing diagnostic information and benefit to all quality measures, especially with the cascade bilateral filter with a Wiener filter and bilateral, nonlocal filter alone. The results of the comparative analysis show that the proposed hybrid framework always outperforms the others in terms of the different quality measures, yielding improved visualization of the lung structures.

Keywords: Bilateral filter, Nonlocal Mean (NLM) filter, Peak Signal-to-Noise Ratio (PSNR), Structural Similarity Index (SSIM), Wiener filter.

1. INTRODUCTION

Noise, poor contrast resolution, and the presence of artifacts that obscure clinically relevant or related features are likely to impact image quality for the diagnosis of pneumonia with chest X-rays (CXR). This study suggests utilizing a strong hybrid preprocessing framework

*Corresponding author
Peer review under the responsibility of University of Baghdad.
https://doi.org/10.31026/j.eng.2026.11.03
This is an open access article under the CC BY 4 license (http://creativecommons.org/licenses/by/4.0/).
Article received: 06/08/2026
Article revised: 01/10/2026
Article accepted: 13/10/2026
Article published: 01/11/2026

that integrates contrast enhancement, structure preservation, classical noise reduction, and learning-based preprocessing approaches into a single model to enhance CXR image quality for diagnosing pneumonia. DAE, symbolizing Denoising Autoencoder, is the learning-based technique utilized. Typical approaches are median filtering, block matching, 3D filtering (BM3D), and Contrast-Limited Adaptive Histogram Equalization (CLAHE). Enhancement studies of chest X-rays in the recent past have shown that dedicated preprocessing pipelines can significantly enhance the contrast, information content and the image diagnostic interpretability, making it crucial to combine the contrast enhancement with the right image preprocessing **(Siracusano et al., 2023).**

In this evaluation study, the CXR images were taken from publicly available CXR datasets for pneumonia to evaluate the effectiveness of each preprocessing technique or combination of preprocessing techniques to improve CXR images for the task of pneumonia detection. Peak signal-to-noise ratio (PSNR), structural similarity index (SSIM), mean squared error (MSE), entropy, and contrast enhancement index (CII) are all used in performance evaluation. The results show that the proposed hybrid approach is able to achieve the greatest performance in the quality of the images generated, in retaining the integrity of the structures in the images, and in improving the contrast in the images when compared with other preprocessing methods **(Priya and Rani, 2026)**.

In a similar manner, CLAHE-based enhancement was integrated into the pneumonia-oriented chest X-ray analysis pipeline, for use in subsequent image classification, where contrast improvement in local regions improved the image's contrast **(Rifa'i et al., 2024).**

Today, in the medical field, X-ray imaging is a widely used tool for the visual diagnosis of a number of medical conditions. This trait makes it essential for the diagnosis of bone fractures, the assessment of lung disease, and the performance of many medical operations, and, because it does not involve injury to the patient, it is a non-invasive technique. In certain situations, however, these scans may not be sufficiently saturated or contrasted, making it difficult for medical experts to make proper interpretations. A novel meta surface optimization method is introduced to improve chest radiographs in this paper. In particular, a preprocessing phase has been added, which performs anisotropic diffusion filtering to remove spot noise. Later, to improve the input parameters for gamma correction and the Contrast-Limited Adaptive Helix Equation (CLAHE), triangulation and topology clustering optimizers (TTAO) are integrated, offering flexibility at various image saturation and contrast levels **(Ramos-Soto et al., 2026)**.

Multilevel CLAHE-derived information has also been explored for low-contrast chest X-ray enhancement to be used for deep contrast diffusion learning **(Anand et al., 2023).**

The 2D multi-stage wavelet inversion (2D-IWT) process completes image reconstruction and removes noise using a hybrid noise reduction approach. Lastly, the PSNR, a measure of image quality, is used to assess and quantify the hybrid system's performance. Experimental evaluations show that the outcomes of the suggested method are approximately 17.5% better than those of previous studies. Instead of employing spatial field filters or multi-resolution wavelet field filters independently, it also enhances the core quality of images in regard to noise reduction and edge preservation **(Ismael and Baykara, 2022)**.

X-ray images of the chest are segmented with high quality. To examine this strategy's effectiveness, the Japan Society of Radiological Technologists (JSRT) dataset, comprising 247 chest X-rays, was utilized. Preprocessing, segmentation, and validation by classification were three stages in which the research was conducted. The novelty of this study lies in the combination of a deblurring autoencoder with a CLAHE, symbolizing constrained adaptive

histogram equalization, for preprocessing; A combined method that combines Kani edge detection with grain segmentation for segmentation, automatic thresholding, Otsu thresholding, and morphology; and GLCM, symbolizing Gray Level Co-occurrence Matrix, to extract features, which helps in classification. Using receiver operating characteristic (ROC) curves and a unique combination of various standard segmentation techniques and classifiers, including XGBoost, nearest neighbor (KNN) algorithm, logistic regression, support vector machine (SVM), naive Bayes, random forest, and decision tree, the quality of lung X-ray image classification as nodules versus non-nodules and malignant versus benign was examined **(Thamilarasi et al., 2025)**.

Preprocessing and image analysis have also been recognized as key issues in medical imaging, as evidenced by recent research. The image preprocessing and enhancement techniques were applied to fundus-image classification **(Ali and Dawood, 2023)** and CLAHE was used as an effective preprocessing stage in the MRI skull stripping **(Nayyef and Al-Tammi, 2023).** Moreover, in recent studies segmentation and classification methods used in brain MRI analysis have been researched and assessed **(Ghadi and Salman, 2022).**

The N-CLAHE method, which uses both local and global enhancement, was suggested as a way to improve the image quality of digital chest radiography. The procedure has two main stages: first, the original image intensity is corrected using a logarithmic normalization function, which dynamically modifies the image intensity contrast. Second, the Adaptive Histogram Equation (CLAHE) procedure is utilized to enhance fine details, local contrast, and texture of the images. Simulation models for both chest and radiographic exams were used to evaluate the suggested method, which was then contrasted with more conventional enhancement techniques like CLAHE, blur masking, and histogram equalization. The outcomes exhibit that the suggested N-CLAHE process achieves significant improvement compared to traditional preprocessing corrections for digital chest radiography **(Koonsanit et al., 2017)**.

Utilizing a standard discrete wavelet transform with an adaptive soft threshold as the noise reduction core, a CUDA-based hybrid wavelet noise reduction application was developed. The suggested implementation joins task-level and data-level parallelism within a unified GPU pipeline and incorporates an integrated reconstruction core, two-stream vertical scrolling scheduling, symmetric boundary processing, persistent memory filter taps, and selective loop opening. Using motion artifacts, simulated Reiki noise, and artificial Gaussian noise, experiments were performed on 3064 * 512,512 grayscale brain MRI images. Further sensitivity analysis was performed to measure the influence of the threshold, filter length, and wavelet basis measurement on runtime, RMSE, SSIM, and PSNR. Whereas computational performance was measured by throughput and runtime, reconstruction quality was assessed using the structural similarity index, the maximum signal-to-noise ratio, and the RMSE **(Hentosh et al., 2026)**.

Wavelet domain denoising remains an active area of research for preserving clinically relevant features while reducing noise, such as optimized wavelet-thresholding methods, and frameworks for wavelet-based chest X-ray restoration **(Benhassine et al., 2021; Song and Ye, 2023).**

Image Noise Reduction Using Wavelet Transforms in Fuzzy Fields: A Review of Recent Advances. Wavelet transforms have become an effective tool for image noise reduction. Thresholding the wavelet parameters is a widely used technique. This research suggests a hybrid noise reduction process combining wavelet transforms, nonlinear diffusion, and median filtering. Furthermore, to reduce additional noise in color digital images, a new fuzzy filter is presented. Two different image noise reduction procedures are reviewed: one uses

a triangular asymmetric moving average (TMAV) filter with a HAAR wavelet transform, whereas the other uses a triangular asymmetric median (TMED) filter with a HAAR wavelet transform **(Agotra and Singhal, 2024)**.

In recent years, with the rapid development of computing and data storage technologies, noise reduction techniques for medical images have seen significant improvement. This is because of the MRA, which symbolizes the emergence of multi-resolution analysis, at both algorithmic and mathematical levels. We suggest, in this research, a hybrid multi-resolution noise reduction approach combining Wiener filters and nonlocal means along with a multi-band decomposition method. Two of the most popular MRA-based decomposition methods, Experimental Wavelet Transform (EWT) and Experimental Mode Decomposition (EMD), were compared. Noise reduction simulations on a sample of reference X-ray images demonstrate the effectiveness of multi-band noise reduction, particularly when the hybrid filtering is combined with EWT. In the coming years, these outcomes provide strong indications of its potential for integration into real-world scanners **(Rabbouch et al., 2022)**. In medical X-ray images, the effectiveness of Wiener-based processing for Poisson-noise reduction has been proven in the past **(Göreke, 2023),** and in chest X-ray tomosynthesis, the effectiveness of NLM-based filtering for noise reduction has been proven in the past **(Park et al., 2022).** Unwanted information that lowers the quality of digital images is called noise. This research aims to remove noise from noisy images using the least-squares method and microwave filters. Methodology/Statistical Analysis: The one-dimensional least-squares method, suggested by Selesnik, was expanded to include noise removal from two-dimensional images. In our proposed approach to formulating the least-squares problem for image noise removal, microwave filter coefficients were used in place of the matrix built using second-order filter coefficients. Results: The technique was applied to standard digital images: Operator, Barbara, Lena, House, and Pepper. These images were exposed to various types of noise, including salt and pepper noise, Gaussian noise, and spot noise, at noise levels (0.01-0.5 dB). The microwave filters utilized in the suggested noise removal method included Haar, Dubichies, Simelt, Quiflet, Bidirectional, and Bidirectional Reverse. The maximum signal-to-noise ratio (PSNR) is used to assess the experimental outcome **(Veena et al., 2016)**.

In recent years, procedures for denoising medical images have seen remarkable improvement. This is because of the advent of Multi-Resolution Analysis (MRA) at algorithmic and mathematical levels. We propose, in this paper, a hybrid procedure to MRA that combines two filters—nonlocal averages and the Wiener filter—with a multiscale analysis method. We conducted a comparative study of two of the most popular MRA-based analysis procedures, EWT and EMD. Simulations of denoising on a set of reference X-ray images proved that MRA was effective, especially when hybrid filtering and EWT were used together. Within the next few years, these outcomes suggest the potential for integrating these techniques into real-world scanners **(Rabbouch et al., 2022)**.

Gaussian, Wiener, and Discrete Wavelet Transform (DWT) filters used for enhancing X-ray images are an effective hybrid framework. In order to find explosives or illegal items, digital X-ray images are essential. However, there are a number of issues with modern X-ray images, including low contrast, noise, and blurring. Pixel intensity and object edges values are affected by noise, leading to ambiguity in object separation and making decision-making difficult. A novel two-layer hybrid framework is proposed to overcome these issues. First, it reads and merges X-ray images that are high- and low-power using different wavelet-domain fusion rules with Discrete Wavelet Transform (DWT), then reconstructs them using

Inverse Discrete Wavelet Transform (iDWT). The combined image is then subjected to a Gaussian filter to eliminate Gaussian noise, followed by a Wiener filter to lessen blurring and enhance image quality. PSNR and MSE values were used to measure image quality. The findings indicate that, in comparison to the original images, the combined images' average PSNR is 10% higher and their MSE is 40% lower. Experimental outcomes indicate that this hybrid frame successfully improves contrast and resolution, and reduces noise and distortion **(Ullah et al., 2023)**.

Recently, deep denoising architectures have been reported to yield enhancement results on chest CT and chest X-ray images on PSNR and SSIM metrics, which accentuates the importance of assessing enhancement techniques using complementary structural and distortion-based metrics **(Nayak et al., 2023).** Digital images are often easily degraded by various types of noise and the complex procedures involved in encoding, acquisition, transmission, retrieval, storage, compression, and so on. Loss of visual information and distortion of image quality are caused by all these factors. Image noise reduction procedures are commonly utilized to solve this issue by removing the different types of noise that are present in the degraded image while maintaining as much detail and important signal characteristics as possible. Wavelet noise reduction seeks to preserve the essential features of the degraded image while eliminating undesired noise. This is made possible by its capacity to split the deteriorated image into four subbands, or sub-images, and work independently on each one's frequencies. For reliable performance, the original image content must be preserved. This work implements and presents a novel hybrid image noise reduction system using Added White Gaussian Noise (AWGN) **(Ismael and Baykara, 2022)**.

Denoising method according to total contrast regularization of chest X-ray images with application to the Nesterov optimization method. A second-order cone programming problem is used to formulate the denoising problem, which is subsequently converted into a saddle point problem with a minimum and a maximum. The Anscombe transform is also used to prepare chest X-ray images for the denoising problem. The Radiopaedia dataset's chest X-ray images were used in the experiments. PSNR and structural similarity metrics are used to assess denoising outcomes. We evaluate the image quality following denoising of the suggested method with other comparable denoising techniques depending on the image quality evaluation metrics. The suggested approach performs better than other comparable noise reduction techniques, according to the results **(Thanh et al., 2020)**.

Several studies have researched the use of contrast enhancement procedures in chest X-ray imaging. One of the most popular methods is Contrast-Limited Adaptive Histogram Equalization (CLAHE), which enhances local contrast while lowering noise amplification. The performance of CLAHE technology is greatly influenced by the "Cutting Threshold" parameter, which controls the degree of contrast enhancement. An inappropriate cutoff threshold may result in under-enhancement or amplification of noise and artifacts. Therefore, choosing the optimal cutoff threshold is crucial to improving the quality of diagnostic images **(Prince et al., 2024)**.

In addition to improving contrast, noise reduction is a crucial step in medical image preprocessing. Bilateral filtering is widely used because it reduces noise while preserving image boundaries by exploiting spatial similarities and intensity between adjacent pixels. The bilateral filtering method has been used in chest X-ray images to enhance the contrast of lung structures and slight pathological changes **(Liu and Nguyen, 2024)**.

Another important noise reduction method is Wiener filtering which minimizes the mean square error between the original and the reconstructed image. It is especially useful in

diminishing Gaussian noise and image quality deterioration, while maintaining the anatomical structure. Recently, the researchers in **(Bian and Yang, 2023; Nia and Shih, 2024)** have used CLAHE in parallel with Wiener filtering for improving chest X-ray images before classification using a deep learning method and obtained good classification accuracy. Nonlocal filtering (NLM) has received considerable attention because it uses the similarity of image components to suppress noise. NLM, on the other hand, maintains the texture and fine details in the image, which makes it good for medical images where fine structure is important in diagnosis. Recent research has shown that combining CLAHE, wavelet transform, and NLM noise reduction can significantly improve the quality and visual interpretation of medical images **(Gamara et al., 2022)**.

This study proposes adaptive work for enhancing chest radiograph quality metrics images that integrate CLAHE and wavelet transform without filters, with filters, and with cascaded noise reduction filters. The proposed work analyzes the influence of the clipping limit and the wavelet transform's K-factor on image quality metrics for a two-class chest radiograph dataset. Enhanced images are evaluated using image quality metrics.

2. Method

The proposed work evaluated the impact of enhancement parameters on image quality metrics independently. Evaluate image quality metrics using one image from each class, consist of two parts, the first one adjust different CLAHE clip limit and wavelet k factor to calculate the image quality metrics for two classes images without using filters, and the second parts using bilateral, Wiener, nonlocal filters and cascade them and then calculate the two classes image quality metrics to see the image enhancement as presented in **Fig. 1**.

2.1 Contrast Limited Adaptive Histogram Equalization (CLAHE)

An improved form of adaptive histogram equalization (AHE) called CLAHE is utilized to enhance local contrast in images without overly enhancing noise. In chest X-rays in particular, CLAHE is widely used in medical imaging because it enhances local contrast, reveals hidden anatomical details, preserves borders, avoids over-enhancement of homogeneous regions, and reduces noise enhancement compared to standard histogram equalization. The development of CLAHE was based on adaptive histogram equalization techniques that were developed to enhance local contrast without over-amplifying the noise in conventional AHE **(Pizer et al., 1987; Zuiderveld, 1994).**

2.2 Wavelet Transform for Image Enhancement

A robust mathematical technique is utilized to analyze signals and images at various resolutions and scales. The wavelet transform simultaneously provides spatial (position) and frequency information. The Fourier transform, on the other hand, solely yields frequency information. In medical image processing, particularly in chest X-ray enhancement, wavelets are widely used because they enhance fine details and edges, preserve important anatomical structures, enable multi-resolution analysis, improve feature extraction for machine learning, and reduce the loss of diagnostic information. The Haar wavelet transform is used because it is simple, computationally efficient, and well-suited for medical image enhancement. The Haar wavelet is the simplest wavelet.

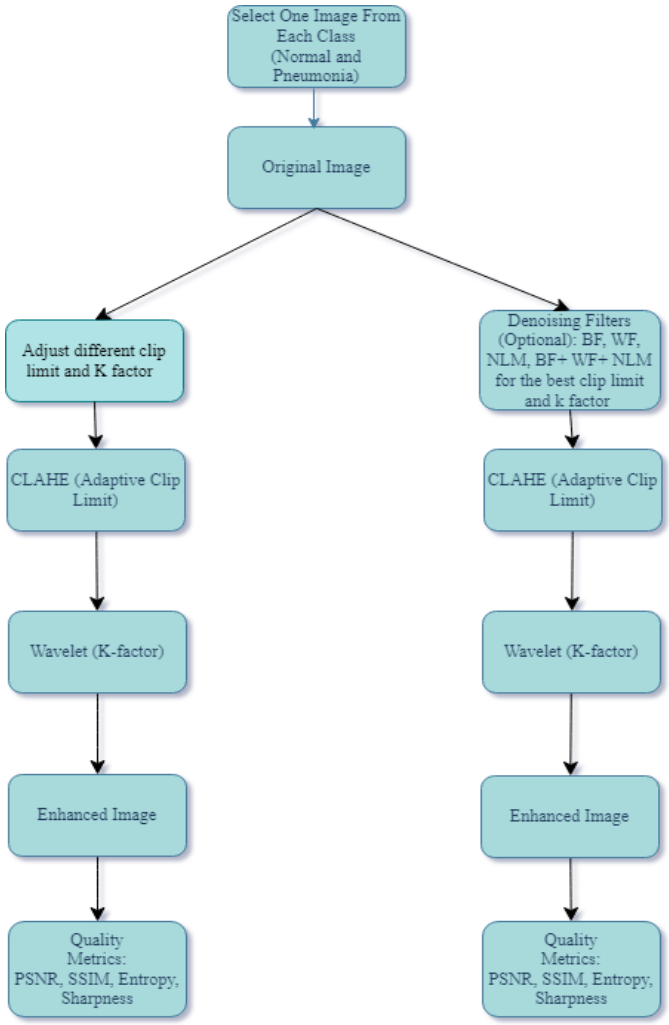


Figure 1. The suggested work.

2.3 Bilateral Filter (BF)

It is a nonlinear, edge-preserving smoothing filter introduced by Carlo Tomasi and Roberto Manduchi in 1998. Unlike standard smoothing filters, the bilateral filter uses both spatial neighborhood and intensity similarity to reduce noise while maintaining high-importance edges. Chest X-ray image enhancement is widely known to use a bilateral filter due to its ability to inhibit noise while preserving important anatomical features like lung boundaries or rib edges **(Tomasi and Manduchi, 1998)**.

2.4 Wiener Filter

Wiener filter is a linear adaptive filter that is used to minimize the mean square error (MSE) between the estimated image and the original image. It adjusts its filtering process based on the local image statistics, which makes it suitable for the additive Gaussian noise removal while maintaining image details. The Wiener filter is widely used in the processing of chest X-rays to remove acquisition noise prior to enhancement or classification purposes **(Buades et al., 2005)**.

2.5 Nonlocal Means

The Nonlocal Means (NLM) filter is an advanced denoising algorithm introduced by Antoni Buades, Bartomeu Coll, and Jean-Michel Morel in 2005. NLM differs from the local filters in estimating each pixel based on weighted averages of all pixels with similar neighborhoods in the image. This nonlocal approach maintains texture and fine anatomical details and is especially well suited for medical imaging **(Gonzalez and Woods, 2018)**.

2.6 Entropy

Entropy measures the quantity of randomness or information held in an image. It indicates how much information is available for visual interpretation, as shown in Eq. (1) **(Pratt, 2007)**. Higher entropy generally means the image contains more details and richer information. For medical images, entropy is often used to evaluate whether an enhancement algorithm has increased the visibility of anatomical structures.

$$H = -\sum_{i=0}^{L-1} p(i) \log_2 p(i) \quad (1)$$

Where $p(i)$ is the probability of gray level, H is the entropy, and L is the number of gray levels (256 for an 8-bit image).

2.7 Peak Signal-to-Noise Ratio

PSNR measures the similarity between the original image and the processed image. It measures how much distortion is presented during enhancement.
The enhanced image is closer to the original image when the PSNR value is higher, as shown in Eqs. (2) and (3) **(Pratt, 2007)**.

$$MSE = \frac{\sum_{i=1}^{M} \sum_{j=1}^{N} [I(i,j) - K(i,j)]^2}{MN} \quad (2)$$

$$PSNR = 10 \log_{10} \left(\frac{MAX^2}{MSE} \right) \quad (3)$$

Where $K(i,j)$ is the enhanced image, $I(i,j)$ is the original image, and MAX = 255 for an 8-bit image.

2.8 Structural Similarity Index (SSIM)

In the image similarity measurement field, SSIM deals with the similarity of images based on luminance, contrast, and structural information together in a single step and is generally applied to compare processed images with reference images **(Wang et al., 2004)**. SSIM is influenced by the region of interest used, and the spatial-frequency properties of the ROI, and should be assessed in conjunction with other complementary image-quality metrics in medical radiographic imaging **(Maruyama, 2023).**

2.9 Contrast

Contrast describes the difference in intensity between neighboring pixels or image regions, as shown in Eqs. (4) and (5) **(Pratt, 2007)**. High contrast improves the visibility of edges and anatomical structures in chest X-ray images.

$$CRMS = \sqrt{\frac{\sum_{i=1}^{M}\sum_{j=1}^{N}(I(i,j)-\mu)^2}{MN}} \quad (4)$$

$$\mu = \frac{\sum_{i=1}^{M}\sum_{j=1}^{N} I(i,j)}{MN} \quad (5)$$

Where μ is the mean intensity.

2.10 Sharpness

Sharpness measures how clearly image edges and fine details are represented. In chest X-ray images, as presented in Eq. (6), higher sharpness improves the pathological regions, lung boundaries, and visibility of ribs. A common measure uses the image gradient as shown in Eq. (7) **(Pratt, 2007)**.

$$Sharpness = \frac{\sum_{i=1}^{M}\sum_{j=1}^{N}\backslash\nabla I(i,j)\backslash}{MN} \quad (6)$$

$$\backslash\nabla I\backslash = \sqrt{\frac{\partial I}{\partial x}^2 + \frac{\partial I}{\partial y}^2} \quad (7)$$

2.11 Noise Variance

Noise variance measures the volume of noise exhibited in an image by quantifying the variation of pixel intensities around the mean. Lower noise variance indicates a cleaner image, as shown in Eq. (8) **(Pratt, 2007)**.

$$\sigma^2 = \frac{\sum_{i=1}^{M}\sum_{j=1}^{N}(I(i,j)-\mu)^2}{MN} \quad (8)$$

Where σ^2 is the noise variance.

3. RESULTS AND DISCUSSION

Three components make up the work's outcome section, which aims to improve the suggested approach. The Chest X-Ray datasets, which include both normal and pneumonia images, are presented in the first section. The second section explains the enhancement images by using the histogram, CLAHE with adaptive clip limit, and wavelet with adaptive k factor to calculate the image quality metrics without using filters. The third section applied the bilateral, Wiener, and nonlocal filters, and the cascade of them to the image (normal, pneumonia) to get quality metrics and compare with the same images without filters.

3.1 Data Set

The dataset of chest X-ray medical images was used for the experiments, as in **(Mooney, 2018)**, which consists of 5216 medical images with a size of 128x128 pixels. The dataset was divided into two parts, with normal medical images being 1341 and pneumonia images being 3875, respectively. **Fig. 2** shows samples of two classes in the image dataset.

3.2 Image Quality Metrics Results without Filters

In this section, two images were randomly selected for each of the two classes from the X-Ray chest dataset, normal and pneumonia images, as shown in **Fig. 3**, and the quality metrics were determined for different clip limits and K factors for each class of the selected images without using filtering.

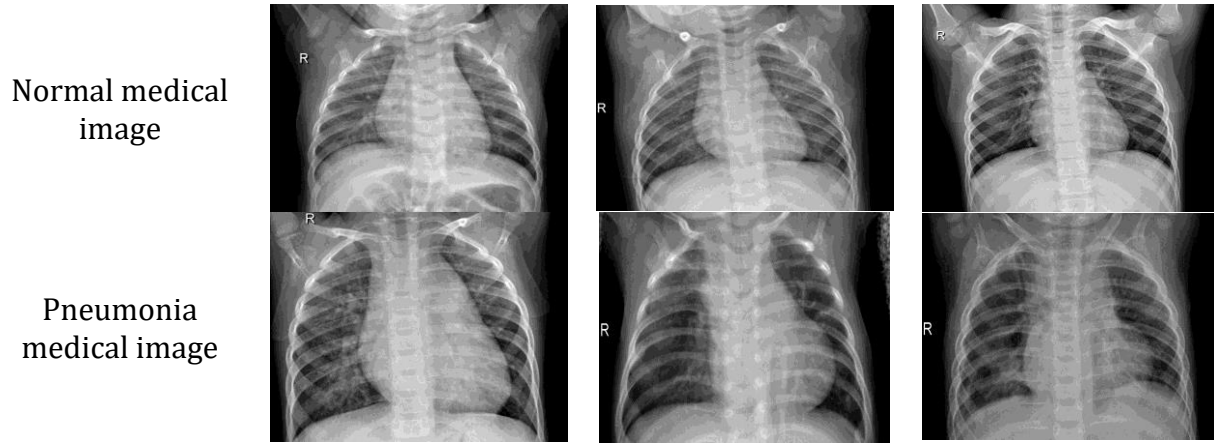


Figure 2. The samples of the two classes' medical dataset.

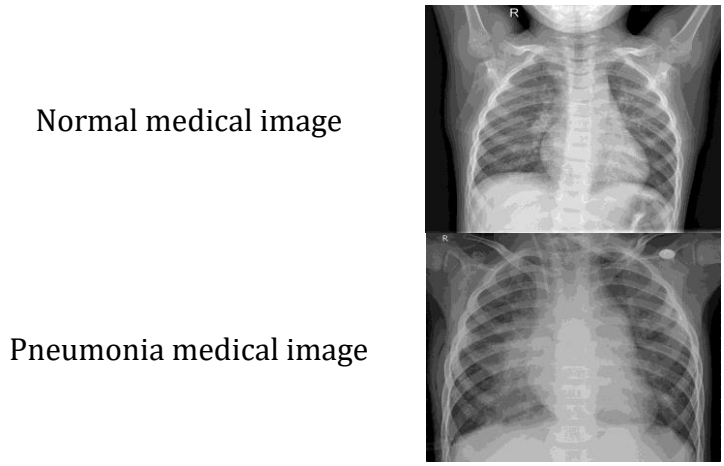


Figure 3. Two image classes were selected randomly.

Tables 1 to 6 illustrate the quality metrics of the normal medical image selected in **Fig. 3** when the K factor was taken to be 1.1 and different clip limits. **Table 1** shows that SSIM and PSNR were better values when compared with other tables when the clip limit was 0.01, as shown in **Fig. 4**, while other metrics (Entropy, contrast, sharpness, and noise variance) had most of their better values at a clip limit of 0.07, as shown in **Table 5** and **Fig. 5**.

Table 1. Quality metrics when clip limit = 0.01.

Medical normal image	Original	CLAHE	Wavelet
Entropy	7.6760	7.5692	5.4941
SSIM	-	0.8032	0.8202
PSNR dB	-	16.6521	16.7133
Contrast	0.2443	0.1837	0.1167
Sharpness	0.0664	0.1320	0.0509
Noise variance	0.059691	0.033729	0.013609

Table 2. Quality metrics when clip limit = 0.02.

Medical normal image	Original	CLAHE	Wavelet
Entropy	7.6760	7.6033	5.5055
SSIM	-	0.7184	0.8167
PSNR dB	-	14.7863	16.6039
Contrast	0.2443	0.1897	0.1159
Sharpness	0.0664	0.1645	0.0530
Noise variance	0.059691	0.035983	0.013438

Table 3. Quality metrics when clip limit = 0.05.

Medical normal image	Original	CLAHE	Wavelet
Entropy	7.6760	7.6317	5.5147
SSIM	-	0.6809	0.8120
PSNR dB	-	13.7894	16.5743
Contrast	0.2443	0.1946	0.1166
Sharpness	0.0664	0.1848	0.0554
Noise variance	0.059691	0.037879	0.013591

Table 4. Quality metrics when clip limit = 0.06.

Medical normal image	Original	CLAHE	Wavelet
Entropy	7.6760	7.6339	5.5123
SSIM	-	0.6791	0.8111
PSNR dB	-	13.7239	16.5792
Contrast	0.2443	0.1949	0.1168
Sharpness	0.0664	0.1866	0.0557
Noise variance	0.059691	0.037998	0.013653

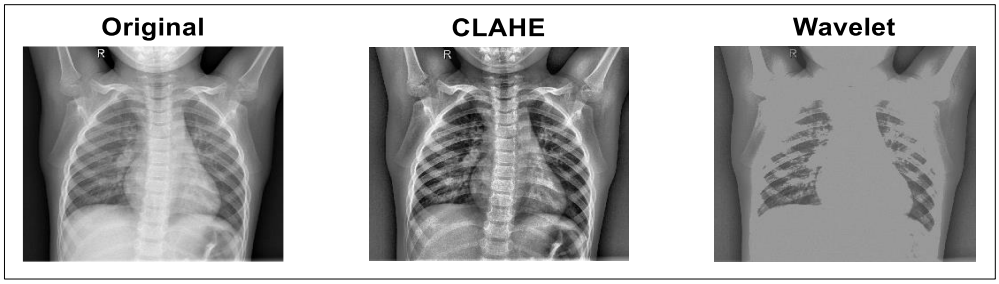
Table 5. Quality metrics when clip limit = 0.07.

Medical normal image	Original	CLAHE	Wavelet
Entropy	7.6760	7.6760	5.5094
SSIM	-	0.6778	0.8102
PSNR dB	-	13.6746	16.5824
Contrast	0.2443	0.1952	0.1171
Sharpness	0.0664	0.1879	0.0560
Noise variance	0.059691	0.038094	0.013721

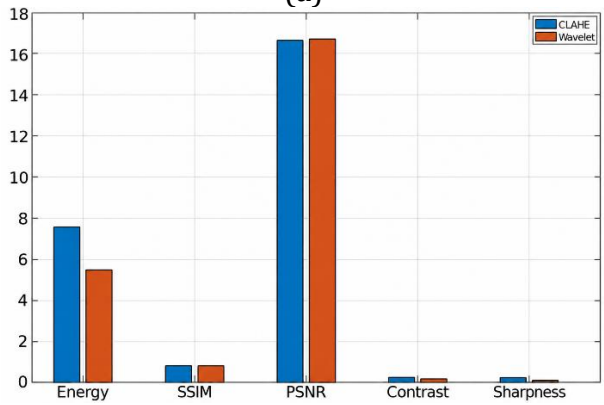
Table 6. Quality metrics when clip limit = 0.09.

Medical normal image	Original	CLAHE	Wavelet
Entropy	7.6760	7.6367	5.5039
SSIM	-	0.6771	0.8084
PSNR dB	-	13.6513	16.5893
Contrast	0.2443	0.1950	0.1178
Sharpness	0.0664	0.1885	0.0566
Noise variance	0.059691	0.038041	0.013880

Tables 7 to 12 illustrate the quality metrics of the normal medical image selected in **Fig. 3** when the K factor was taken to be 1.2 and different clip limits. **Table 7** shows that SSIM and PSNR were better values when compared with other tables when the clip limit was 0.01, as shown in **Fig. 6**, while other metrics (Entropy, contrast, sharpness, and noise variance) had most of their better values at a clip limit equal to 0.09 in **Table 12**, as shown in **Fig. 7**.

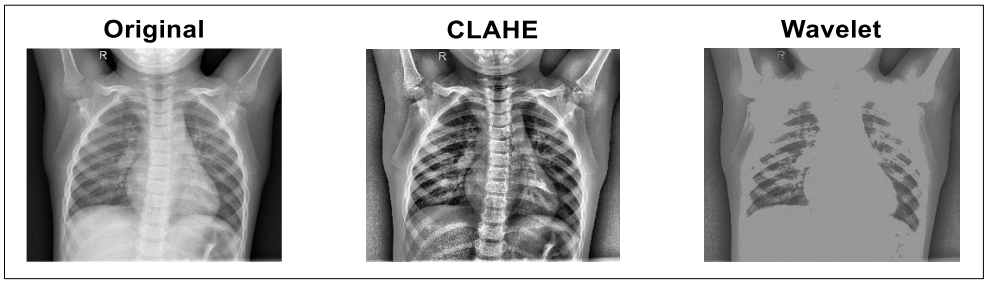


(a)

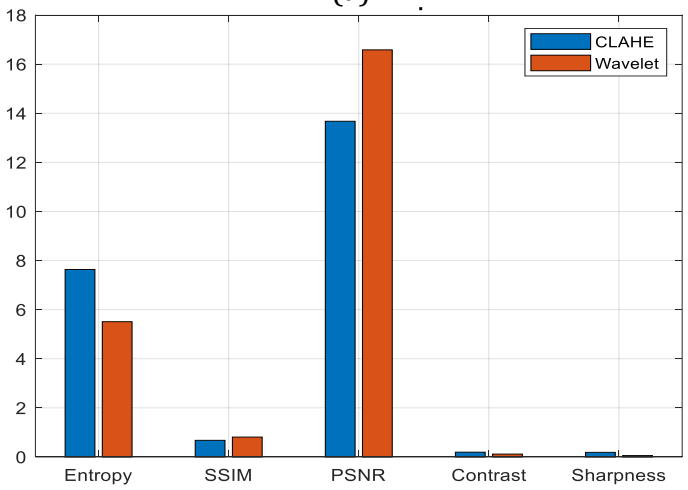


(b)

Figure 4. Appling CLAHE and Wavelet on the original image; (a) normal image with k =1.1, clip limit = 0.01, (b) enhancement parameters.



(a)



(b)

Figure 5. Appling CLAHE and Wavelet on the original image; (a) the normal image with k = 1.1, clip limit = 0.07, (b) the enhancement parameters.

Table 7. Quality metrics when clip limit = 0.01.

Medical normal image	Original	CLAHE	Wavelet
Entropy	7.6760	7.5692	5.4250
SSIM	-	0.8032	0.8194
PSNR dB	-	16.6521	16.2674
Contrast	0.2443	0.1837	0.1064
Sharpness	0.0664	0.1320	0.0483
Noise variance	0.059691	0.033729	0.011321

Table 8. Quality metrics when clip limit = 0.02.

Medical normal image	Original	CLAHE	Wavelet
Entropy	7.6760	7.6033	5.4383
SSIM	-	0.7184	0.8164
PSNR dB	-	14.7863	16.1760
Contrast	0.2443	0.1897	0.1058
Sharpness	0.0664	0.1645	0.0503
Noise variance	0.059691	0.035983	0.011202

Table 9. Quality metrics when clip limit = 0.05.

Medical normal image	Original	CLAHE	Wavelet
Entropy	7.6760	7.6317	5.4487
SSIM	-	0.6809	0.8121
PSNR dB	-	13.7894	16.1444
Contrast	0.2443	0.1946	0.1065
Sharpness	0.0664	0.1848	0.0525
Noise variance	0.059691	0.037879	0.011347

Table 10. Quality metrics when clip limit = 0.06.

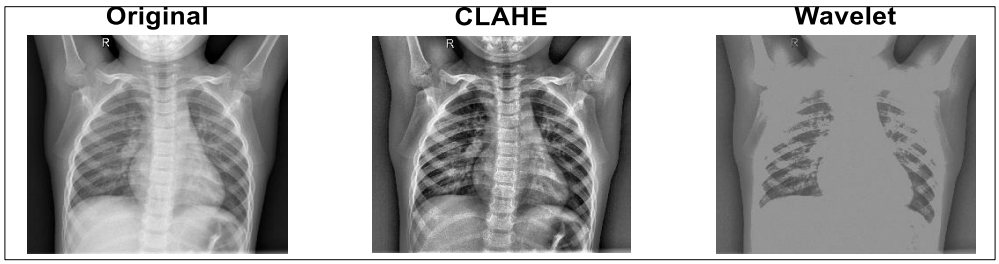
Medical normal image	Original	CLAHE	Wavelet
Entropy	7.6760	7.6339	5.4461
SSIM	-	0.6791	0.8112
PSNR dB	-	13.7239	16.1442
Contrast	0.2443	0.1949	0.1068
Sharpness	0.0664	0.1866	0.0527
Noise variance	0.059691	0.037998	0.011397

Table 11. Quality metrics when clip limit = 0.07.

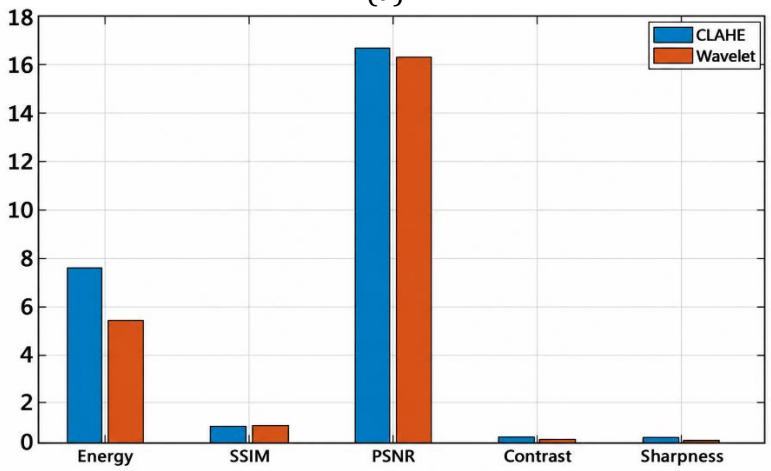
Medical normal image	Original	CLAHE	Wavelet
Entropy	7.6760	7.6363	5.4432
SSIM	-	0.6778	0.8103
PSNR dB	-	13.6746	16.1428
Contrast	0.2443	0.1952	0.1070
Sharpness	0.0664	0.1879	0.0530
Noise variance	0.059691	0.038094	0.011453

Table 12. Quality metrics when clip limit = 0.09.

Medical normal image	Original	CLAHE	Wavelet
Entropy	7.6760	7.6367	5.4375
SSIM	-	0.6771	0.8085
PSNR dB	-	13.6513	16.1441
Contrast	0.2443	0.1950	0.1076
Sharpness	0.0664	0.1885	0.0536
Noise variance	0.059691	0.038041	0.011583

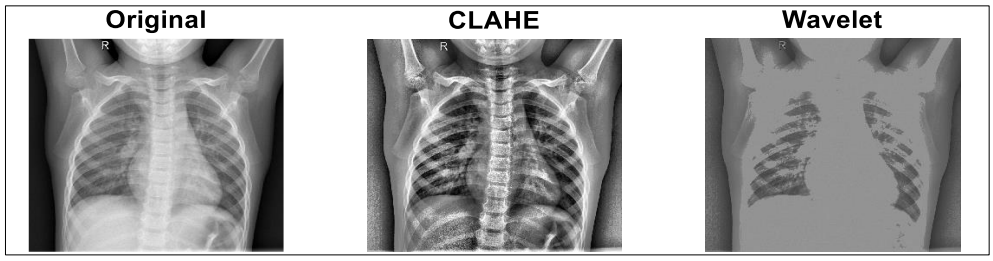


(a)

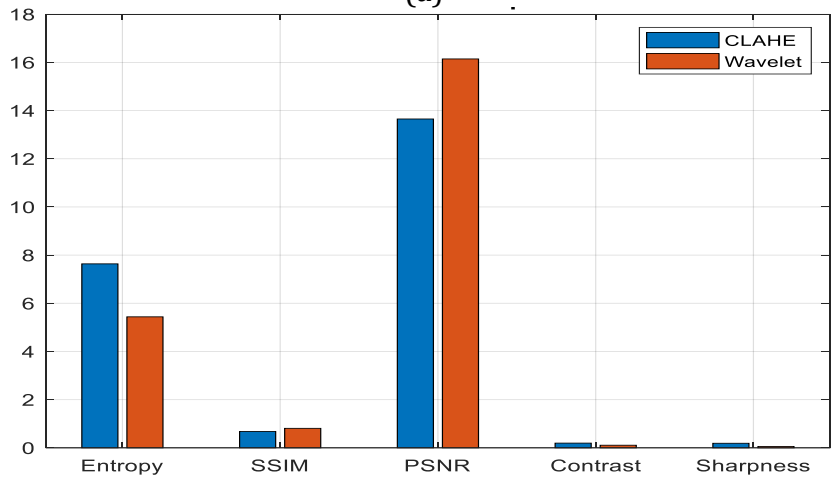


(b)

Figure 6. Appling CLAHE and Wavelet on the original image; (a) the normal image with k =1.2, clip limit = 0.01, (b) the enhancement parameters.



(a)



(b)

Figure 7. Appling CLAHE and Wavelet on the original image; (a) the normal image with k = 1.2, clip limit = 0.09, (b) the enhancement parameters.

Tables 13 to 18 illustrate the quality metrics of the normal medical image selected in **Fig. 3** when the K factor was taken to be 1.3 and different clip limits. **Table 13** shows that SSIM and PSNR were better values when compared with other tables when the clip limit was 0.01, as shown in **Fig. 8**, while other metrics (Entropy, contrast, sharpness, and noise variance) had most of their better values at a clip limit of 0.07 in **Table 18**, as shown in **Fig. 9**. **Tables 19 to 24** illustrated the quality metrics of the pneumonia medical image in **Fig. 3** when the K factor = 1.1 at different clip limits.

Table 13. Quality metrics when clip limit = 0.01.

Medical normal image	Original	CLAHE	Wavelet
Entropy	7.6760	7.5692	5.3595
SSIM	-	0.8032	0.8179
PSNR dB	-	16.6521 dB	15.8699
Contrast	0.2443	0.1837	0.0976
Sharpness	0.0664	0.1320	0.0460
Noise variance	0.059691	0.033729	0.009530

Table 14. Quality metrics when clip limit = 0.02.

Medical normal image	Original	CLAHE	Wavelet
Entropy	7.6760	7.6033	5.3726
SSIM	-	0.7184	0.8153
PSNR dB	-	14.7863	15.7886
Contrast	0.2443	0.1897	0.0971
Sharpness	0.0664	0.1645	0.0479
Noise variance	0.059691	0.035983	0.009426

Table 15. Quality metrics when clip limit = 0.05.

Medical normal image	Original	CLAHE	Wavelet
Entropy	7.6760	7.6317	5.3853
SSIM		0.6809	0.8114
PSNR dB		13.7894	15.7571
Contrast	0.2443	0.1946	0.0979
Sharpness	0.0664	0.1848	0.0499
Noise variance	0.059691	0.037879	0.009579

Table 16. Quality metrics when clip limit = 0.06.

Medical normal image	Original	CLAHE	Wavelet
Entropy	7.6760	7.6339	5.3838
SSIM	-	0.6791	0.8106
PSNR dB	-	13.7239	15.7548
Contrast	0.2443	0.1949	0.0981
Sharpness	0.0664	0.1866	0.0502
Noise variance	0.059691	0.037998	0.009632

Table 17. Quality metrics when clip limit = 0.07.

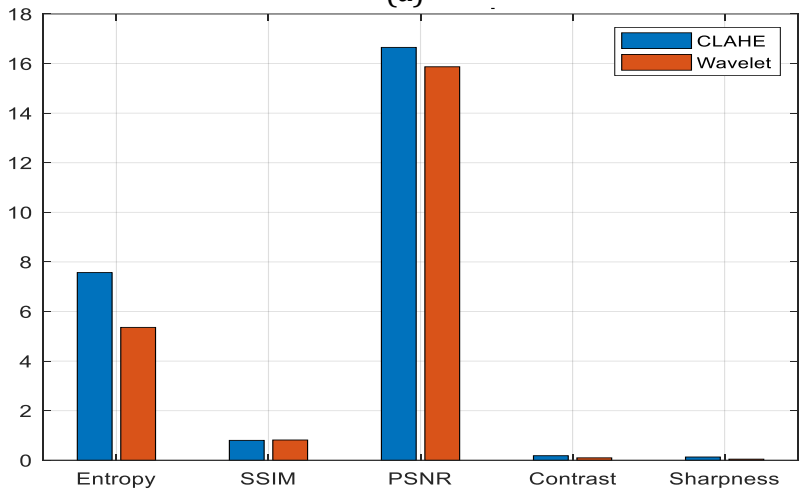
Medical normal image	Original	CLAHE	Wavelet
Entropy	7.6760	7.6363	5.3814
SSIM	-	0.6778	0.8098
PSNR dB	-	13.6746	15.7512
Contrast	0.2443	0.1952	0.0984
Sharpness	0.0664	0.1879	0.0505
Noise variance	0.059691	0.038094	0.009689

Table 18. Quality metrics when clip limit = 0.09.

Medical normal image	Original	CLAHE	Wavelet
Entropy	7.6760	7.6367	5.3767
SSIM		0.6771	0.8080
PSNR dB		13.6513	15.7493
Contrast	0.2443	0.1950	0.0991
Sharpness	0.0664	0.1885	0.0511
Noise variance	0.059691	0.038041	0.009814

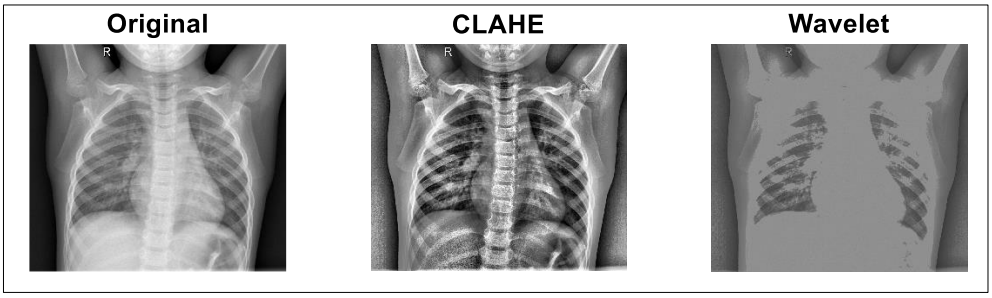


(a)

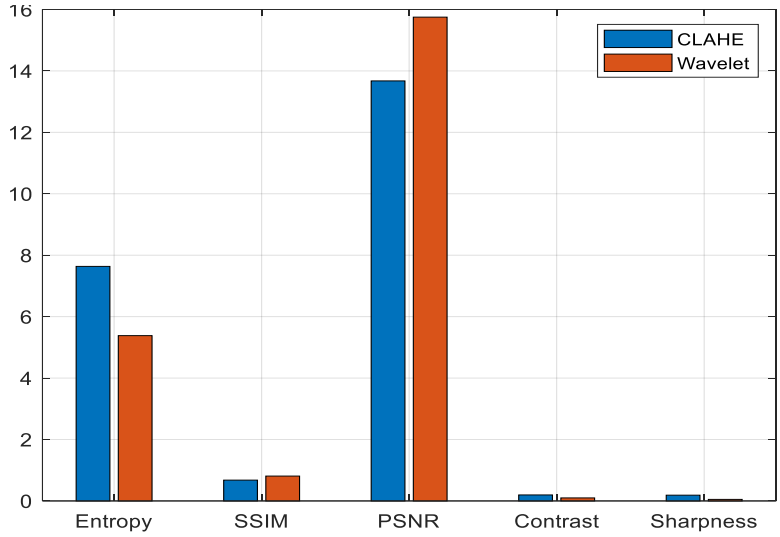


(b)

Figure 8. Appling CLAHE and Wavelet on the original image; (a) the normal image with k = 1.3, clip limit = 0.01, (b)the enhancement parameters.



(a)



(b)

Figure 9. Appling CLAHE and Wavelet on the original image; (a) the normal image with k = 1.3, clip limit = 0.07, (b) the enhancement parameters.

Table 19. Quality metrics when clip limit = 0.01.

Medical pneumonia image	Original	CLAHE	Wavelet
Entropy	7.3712	7.4083	5.7206
SSIM	-	0.8443	0.8997
PSNR dB	-	20.1553	21.0716
Contrast	0.1784	0.1673	0.1100
Sharpness	0.0857	0.1725	0.0758
Noise variance	0.031833	0.027999	0.012104

Table 20. Quality metrics when clip limit = 0.02.

Medical pneumonia image	Original	CLAHE	Wavelet
Entropy	7.3712	7.5960	5.6878
SSIM	-	0.7214	0.8976
PSNR dB	-	17.6712	20.8683
Contrast	0.1784	0.1883	0.1073
Sharpness	0.0857	0.2339	0.0748
Noise variance	0.031833	0.035470	0.011506

Table 21. Quality metrics when clip limit = 0.05.

Medical pneumonia image	Original	CLAHE	Wavelet
Entropy	7.3712	7.6474	5.6633
SSIM	-	0.6636	0.8947
PSNR dB	-	16.3013	20.7429
Contrast	0.1784	0.1953	0.1061
Sharpness	0.0857	0.2743	0.0745
Noise variance	0.031833	0.038124	0.011250

Table 19 shows that SSIM and PSNR were better values when compared with other tables when the clip limit was 0.01, as shown in **Fig. 10**. Other metrics (Entropy, contrast, sharpness, and noise variance) had most of them were better values at a clip limit equal to 0.09 at **Table 24**, as shown in **Fig.11**.

Table 22. Quality metrics when clip limit = 0.06.

Medical pneumonia image	Original	CLAHE	Wavelet
Entropy	7.3712	7.6519	5.6622
SSIM		0.6603	0.8937
PSNR dB		16.1745	20.7448
Contrast	0.1784	0.1958	0.1064
Sharpness	0.0857	0.2748	0.0748
Noise variance	0.031833	0.038344	0.011316

Table 23. Quality metrics when clip limit = 0.07.

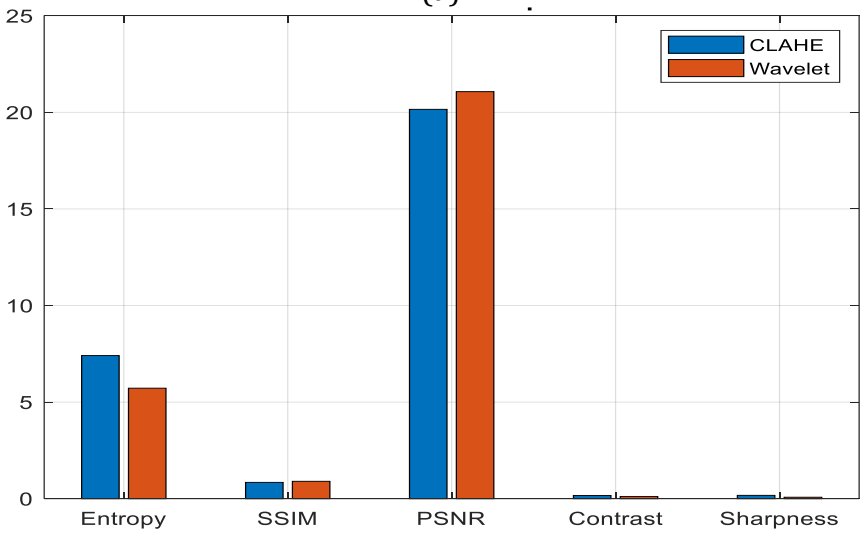
Medical pneumonia image	Original	CLAHE	Wavelet
Entropy	7.3712	7.6527	5.6595
SSIM	-	0.6588	0.8927
PSNR dB	-	16.1205	20.7373
Contrast	0.1784	0.1960	0.1066
Sharpness	0.0857	0.2801	0.0750
Noise variance	0.031833	0.038417	0.011362

Table 24. Quality metrics when clip limit = 0.09.

Medical pneumonia image	Original	CLAHE	Wavelet
Entropy	7.3712	7.6528	5.6552
SSIM	-	0.6583	0.8906
PSNR dB	-	16.1048	20.7383
Contrast	0.1784	0.1961	0.1072
Sharpness	0.0857	0.2806	0.0755
Noise variance	0.031833	0.038437	0.011491



(a)



(b)

Figure 10. Appling CLAHE and Wavelet on the original image; (a) the pneumonia image with k = 1.1, clip limit = 0.01, (b) the enhancement parameters.

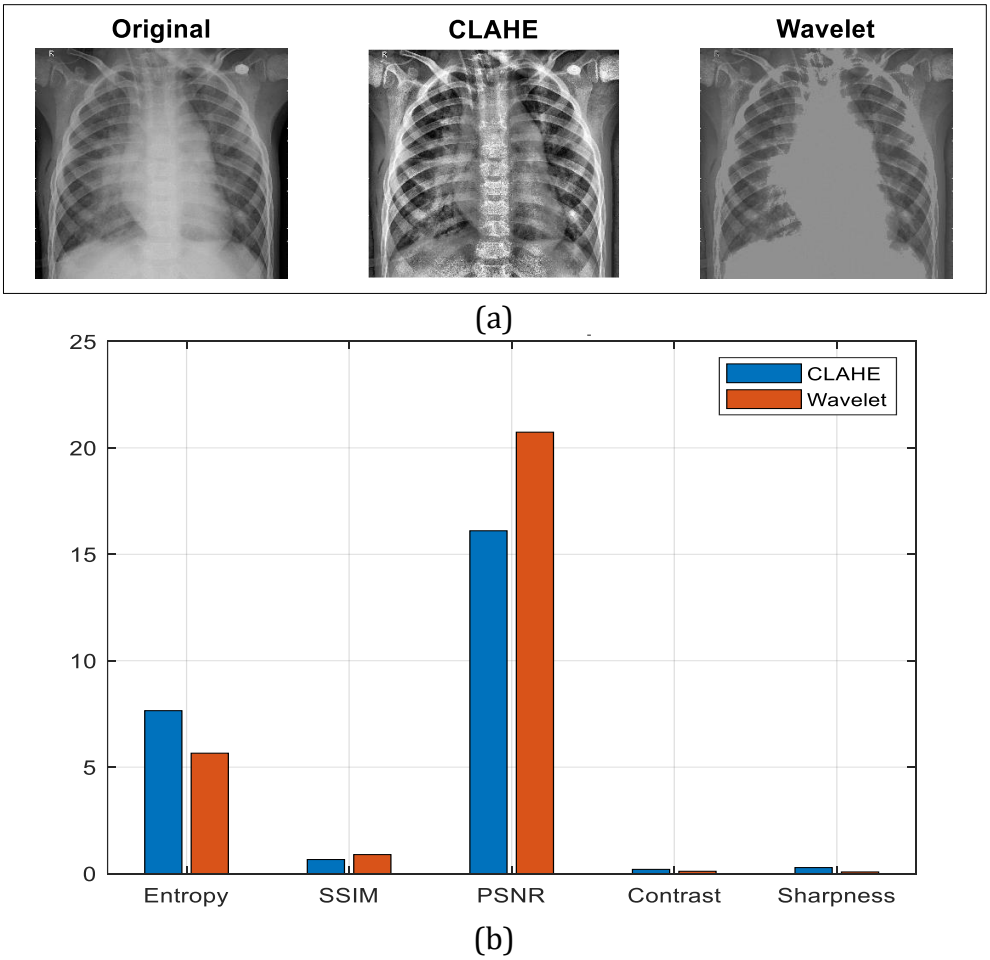


Figure 11. Appling CLAHE and Wavelet on the original image; (a) the pneumonia image with k = 1.1, clip limit = 0.09, (b) the enhancement parameters.

Tables 25 to 30 illustrate the quality metrics of the pneumonia medical image in **Fig. 3** when the K factor = 1.2 at different clip limits. **Table 25** shows that SSIM and PSNR were better values when compared with other tables when the clip limit was 0.01, as shown in **Fig. 12**. Other metrics (Entropy, contrast, sharpness, and noise variance) were mostly better values at a clip limit equal to 0.09 in **Table 30**, as shown in **Fig. 13**.

Table 25. Quality metrics when clip limit = 0.01.

Medical pneumonia image	Original	CLAHE	Wavelet
Entropy	7.3712	7.4083	5.6416
SSIM	-	0.8443	0.9004
PSNR dB	-	20.1553	20.3749
Contrast	0.1784	0.1673	0.1008
Sharpness	0.0857	0.1725	0.0711
Noise variance	0.031833	0.027999	0.010168

Table 26. Quality metrics when clip limit = 0.02.

Medical pneumonia image	Original	CLAHE	Wavelet
Entropy	7.3712	7.5960	5.6087
SSIM	-	0.7214	0.8984
PSNR dB	-	17.6712	20.2354
Contrast	0.1784	0.1883	0.0985
Sharpness	0.0857	0.2339	0.0703
Noise variance	0.031833	0.035470	0.009705

Table 27. Quality metrics when clip limit = 0.05.

Medical pneumonia image	Original	CLAHE	Wavelet
Entropy	7.3712	7.6474	5.5960
SSIM	-	0.6636	0.8957
PSNR dB	-	16.3013	20.1251
Contrast	0.1784	0.1953	0.0980
Sharpness	0.0857	0.2743	0.0704
Noise variance	0.031833	0.038124	0.009614

Table 28. Quality metrics when clip limit = 0.06.

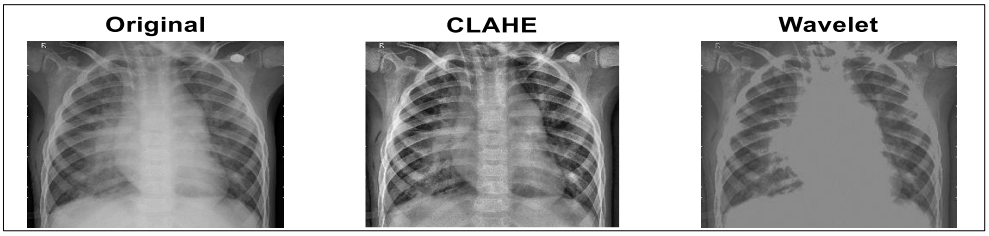
Medical pneumonia image	Original	CLAHE	Wavelet
Entropy	7.3712	7.6519	5.5944
SSIM	-	0.6603	0.8947
PSNR dB	-	16.1745	20.1225
Contrast	0.1784	0.1958	0.0983
Sharpness	0.0857	0.2784	0.0707
Noise variance	0.031833	0.038344	0.009670

Table 29. Quality metrics when clip limit = 0.07.

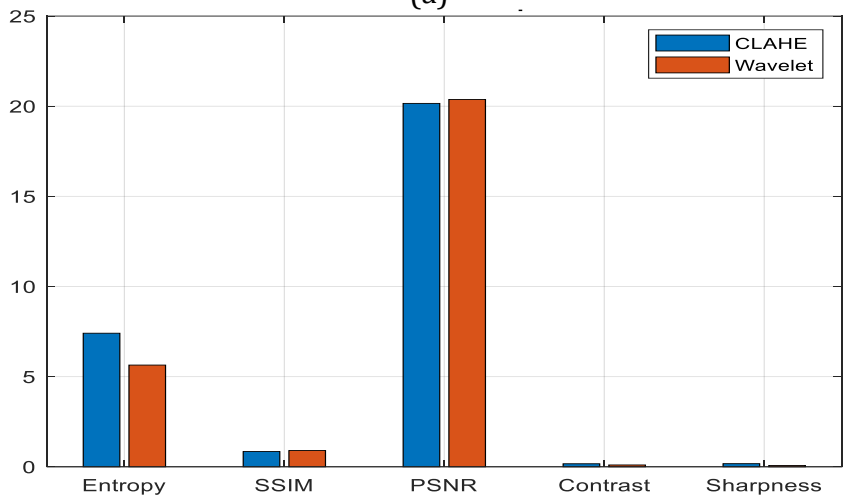
Medical pneumonia image	Original	CLAHE	Wavelet
Entropy	7.3712	7.6527	5.5921
SSIM	-	0.6588	0.8936
PSNR dB	-	16.1205	20.1077
Contrast	0.1784	0.1960	0.0985
Sharpness	0.0857	0.2801	0.0709
Noise variance	0.031833	0.038417	0.009710

Table 30. Quality metrics when clip limit = 0.09.

Medical pneumonia image	Original	CLAHE	Wavelet
Entropy	7.3712	7.6528	5.5877
SSIM		0.6583	0.8915
PSNR dB		16.1048	20.0977
Contrast	0.1784	0.1961	0.0991
Sharpness	0.0857	0.2806	0.0714
Noise variance	0.031833	0.038437	0.009820



(a)

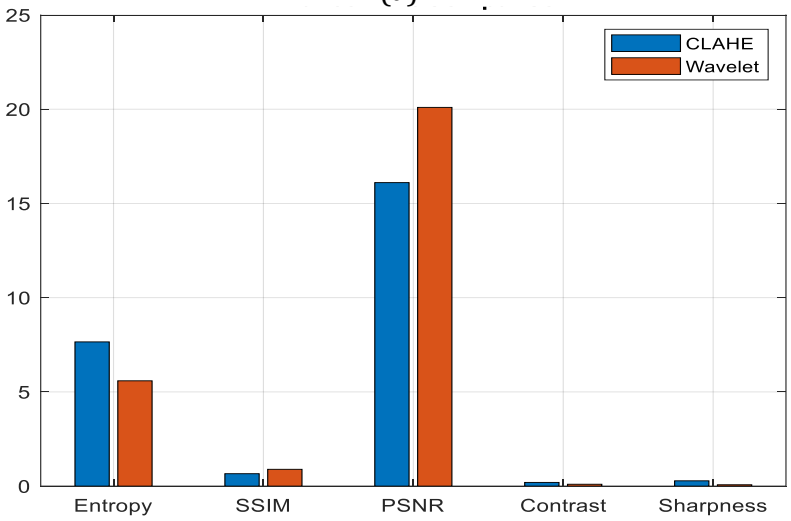


(b)

Figure 12. Appling CLAHE and Wavelet on the original image; (a) the pneumonia image with k = 1.2, clip limit = 0.01, (b) the enhancement parameters.



(a)



(b)

Figure 13. Appling CLAHE and Wavelet on the original image; (a) the pneumonia image with k = 1.2, clip limit = 0.09, (b) enhancement parameters.

Tables 31 to 36 illustrate the quality metrics of the pneumonia medical image in **Fig. 3** when the K factor was set to 1.3 at different clip limits.

Table 31. Quality metrics when clip limit = 0.01.

Medical pneumonia image	Original	CLAHE	Wavelet
Entropy	7.3712	7.4083	5.5671
SSIM	-	0.8443	0.8998
PSNR dB	-	20.1553	19.7550
Contrast	0.1784	0.1673	0.0931
Sharpness	0.0857	0.1725	0.0672
Noise variance	0.031833	0.027999	0.008665

Table 32. Quality metrics when clip limit = 0.02.

Medical pneumonia image	Original	CLAHE	Wavelet
Entropy	7.3712	7.5960	5.5386
SSIM	-	0.7214	0.8978
PSNR dB	-	17.6712	19.6609
Contrast	0.1784	0.1883	0.0911
Sharpness	0.0857	0.2339	0.0665
Noise variance	0.031833	0.035470	0.008299

Table 33. Quality metrics when clip limit = 0.05.

Medical pneumonia image	Original	CLAHE	Wavelet
Entropy	7.3712	7.6474	5.5247
SSIM	-	0.6636	0.8952
PSNR dB	-	16.3013	19.5590
Contrast	0.1784	0.1953	0.0907
Sharpness	0.0857	0.2743	0.0667
Noise variance	0.031833	0.038124	0.008228

Table 31 shows that SSIM and PSNR were better values when compared with other tables when the clip limit was 0.01, as shown in **Fig. 14**. Other metrics (Entropy, contrast, sharpness, and noise variance) had most of their values better at a clip limit of 0.09 in **Table 36**, as shown in **Fig. 15**.

Table 34. Quality metrics when clip limit = 0.06.

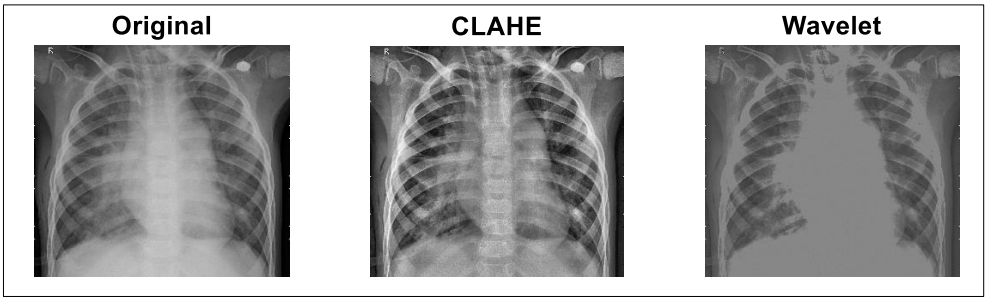
Medical pneumonia image	Original	CLAHE	Wavelet
Entropy	7.3712	7.6519	5.5238
SSIM	-	0.6603	0.8942
PSNR dB	-	16.1745	19.5552
Contrast	0.1784	0.1958	0.0910
Sharpness	0.0857	0.2784	0.0669
Noise variance	0.031833	0.038344	0.008275

Table 35. Quality metrics when clip limit = 0.07.

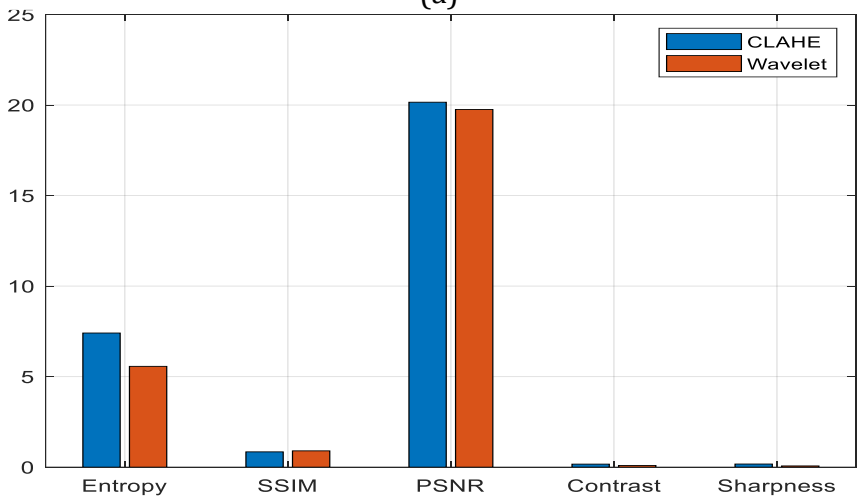
Medical pneumonia image	Original	CLAHE	Wavelet
Entropy	7.3712	7.6527	5.5207
SSIM	-	0.6588	0.8932
PSNR dB	-	16.1205	19.5393
Contrast	0.1784	0.1960	0.0912
Sharpness	0.0857	0.2801	0.0671
Noise variance	0.031833	0.038417	0.008310

Table 36. Quality metrics when clip limit = 0.09.

Medical pneumonia image	Original	CLAHE	Wavelet
Entropy	7.3712	7.6528	5.5163
SSIM	-	0.6583	0.8911
PSNR dB	-	16.1048	19.5268
Contrast	0.1784	0.1961	0.0917
Sharpness	0.0857	0.2806	0.0676
Noise variance	0.031833	0.038437	0.008404

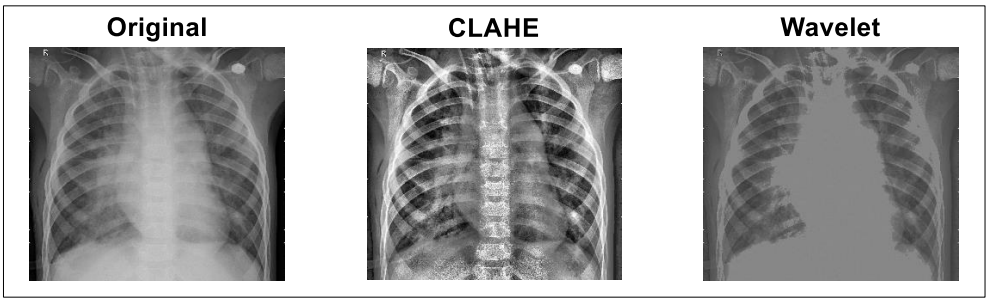


(a)

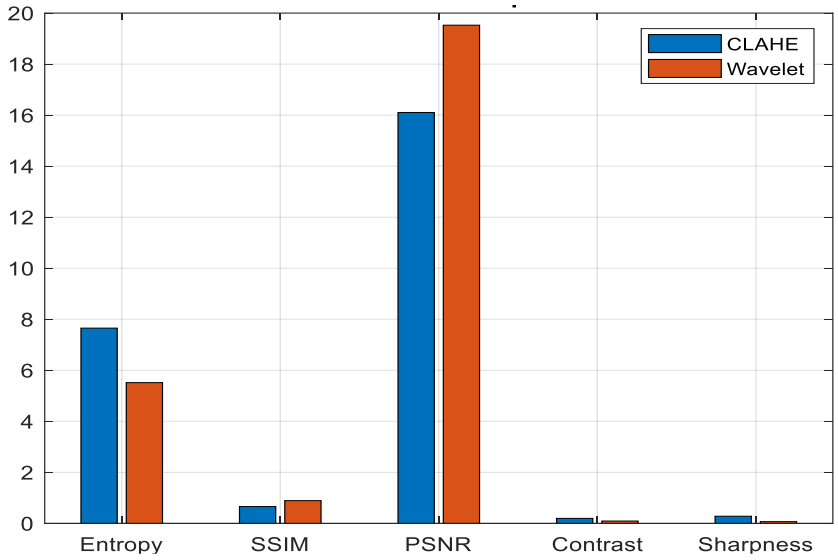


(b)

Figure 14. Appling CLAHE and Wavelet on the original image; (a) the pneumonia image with k = 1.3, clip limit = 0.01, (b) the enhancement parameters.



(a)



(b)

Figure 15. Appling CLAHE and Wavelet on the original image; (a) the pneumonia image with k = 1.3, clip limit = 0.07, (b) the enhancement parameters.

3.2 Image Quality Metrics Results with Filters

In this section, two images were randomly selected for each of the two classes from the X-Ray chest dataset, normal and pneumonia images, as shown in **Fig. 3**, and the quality metrics were determined for different clip limits and K factors for each class of the selected images with filtering (bilateral, Wiener, nonlocal, and cascade of them).

In all processing, later select a clip limit of 0.01 for k = 1.1 for two categories to show the difference between the applied filters and without them, as a sample of other cases of clip limit and k factor. In **Table 37**, the bilateral filter was applied to the normal medical image, as shown in **Fig. 3**, before inputting it to CLAHE and the wavelet transform.

Table 37. Bilateral filter image input it into the CLAHE and wavelet transform.

Medical normal image	Bilateral image	CLAHE	Wavelet
Entropy	7.6270	7.5614	4.2071
SSIM	-	0.8919	0.8813
PSNR dB	-	17.4546	17.1064
Contrast	0.2423	0.1839	0.1204
Sharpness	0.0215	0.0367	0.0143
Noise variance	0.058727	0.033816	0.014504

In **Table 38** shown applied the wiener filter to the normal medical image as shown in **Fig. 3** before inputting it into the CLAHE and wavelet transform at the same clip limit and k factor.

Table 38. Wiener filter image input it to the CLAHE and wavelet transform.

Medical normal image	Wiener image	CLAHE	Wavelet
Entropy	7.6661	7.5644	4.7312
SSIM	-	0.8389	0.8346
PSNR dB	-	16.7943	16.7298
Contrast	0.2441	0.1831	0.1166
Sharpness	0.0474	0.0911	0.0314
Noise variance	0.059599	0.033508	0.013604

In **Table 39**, a nonlocal filter was applied to the normal medical image, as shown in **Fig. 3**, before inputting it to the CLAHE and wavelet transform at the same clip limit and k factor.

Table 39. Nonlocal filter image input to the CLAHE and wavelet transform.

Medical normal image	Nonlocal image	CLAHE	Wavelet
Entropy	7.6693	7.5702	5.4961
SSIM	-	0.8077	0.8218
PSNR dB	-	16.6884	16.7838
Contrast	0.2443	0.1839	0.1177
Sharpness	0.0630	0.1248	0.0465
Noise variance	0.059690	0.033834	0.013855

In **Table 40**, a bilateral plus Nonlocal image filter was applied to the normal medical image, as shown in **Fig. 3**, before inputting it into the CLAHE and wavelet transform at the same clip limit and k factor.

Table 40. Bilateral plus nonlocal image input it into the CLAHE and wavelet transform.

Medical normal image	Bilateral plus non-local image filters	CLAHE	Wavelet
Entropy	7.6270	7.5613	4.2014
SSIM	-	0.8920	0.8813
PSNR dB	-	17.4553	17.1068
Contrast	0.2423	0.1839	0.1204
Sharpness	0.0215	0.0366	0.0142
Noise variance	0.058727	0.033813	0.014505

In **Table 41**, a bilateral plus Wiener image filter was applied to the normal medical image, as shown in **Fig. 3**, before inputting it into the CLAHE and wavelet transform at the same clip limit and k factor.

Table 41. Bilateral plus Wiener image input it into the CLAHE and wavelet transform.

Medical normal image	Bilateral plus Wiener image	CLAHE	Wavelet
Entropy	7.6255	7.5611	4.0354
SSIM	-	0.8930	0.8819
PSNR dB	-	17.4681	17.1072
Contrast	0.2423	0.1840	0.1204
Sharpness	0.0208	0.0354	0.0133
Noise variance	0.058724	0.033839	0.014507

In **Table 42**, the bilateral filter was applied to the pneumonia image as shown in **Fig. 3** before inputting it into the CLAHE and wavelet transform.

Table 42. Bilateral filter image input it into the CLAHE and wavelet transform.

Medical pneumonia image	Bilateral image	CLAHE	Wavelet
Entropy	7.3122	7.3604	5.1061
SSIM	-	0.9421	0.9437
PSNR dB	-	21.1589	20.5034
Contrast	0.1752	0.1627	0.1174
Sharpness	0.0270	0.0468	0.0266
Noise variance	0.030693	0.026460	0.013790

In **Table 43**, the Wiener filter was applied to the medical pneumonia image, as shown in **Fig. 3**, before inputting it in the CLAHE and wavelet transform at the same clip limit and k factor.

Table 43. Wiener filter image input to the CLAHE and wavelet transform.

Medical pneumonia image	Wiener image	CLAHE	Wavelet
Entropy	7.3579	7.3945	5.2568
SSIM	-	0.8855	0.9156
PSNR dB	-	20.4197	20.0535
Contrast	0.1781	0.1664	0.1095
Sharpness	0.0600	0.1166	0.0531
Noise variance	0.031704	0.027689	0.011987

In **Table 44**, a nonlocal filter was applied to the medical pneumonia image, as shown in **Fig. 3**, before inputting it to the CLAHE and wavelet transform at the same clip limit and k factor.

Table 44. Nonlocal filter image input to the CLAHE and wavelet transform.

Medical pneumonia image	Nonlocal image	CLAHE	Wavelet
Entropy	7.3699	7.4071	5.7215
SSIM	-	0.8446	0.8998
PSNR dB	-	20.1762	21.1009
Contrast	0.1784	0.1673	0.1102
Sharpness	0.0856	0.1721	0.0756
Noise variance	0.031834	0.028004	0.012154

In **Table 45**, a bilateral plus nonlocal image filter was applied to a medical pneumonia image, as shown in **Fig. 3**, before inputting it to the CLAHE and wavelet transform at the same clip limit and k factor.

Table 45. Bilateral plus nonlocal image input it into the CLAHE and wavelet transform.

Medical pneumonia image	Bilateral plus nonlocal image filters	CLAHE	Wavelet
Entropy	7.3124	7.3582	5.0888
SSIM	-	0.9420	0.9436
PSNR dB	-	21.1583	20.4974
Contrast	0.1752	0.1626	0.1174
Sharpness	0.0270	0.0468	0.0266
Noise variance	0.030694	0.026447	0.013782

In **Table 46**, a bilateral plus Wiener image filter was applied to the medical pneumonia image, as shown in **Fig. 3**, before inputting it into the CLAHE and wavelet transform at the same clip limit and k factor.

Table 46. Bilateral plus Wiener image input it to the CLAHE and wavelet transform.

Medical pneumonia image	Bilateral plus Wiener image	CLAHE	Wavelet
Entropy	7.3096	7.3560	4.9137
SSIM	-	0.9433	0.9447
PSNR dB	-	21.1388	20.6065
Contrast	0.1752	0.1626	0.1167
Sharpness	0.0254	0.0438	0.0247
Noise variance	0.030692	0.026434	0.013613

Summary **Table 47** compared results between CLAHE and Wavelet transform without filters and with filters for medical normal image when k factor equal 1.1 and clip limit equal 0.01 as shown in **Table 47** that the enhancement of quality metrics gave the high values in entropy when used nonlocal image filter, (SSIM, PSNR, contrast) when used Bilateral cascade wiener filter image, and low value in noise variance when used wiener image filter.
Summary **Table 48** compared results between CLAHE and Wavelet transform without filters and with filters for medical pneumonia image when k factor equal 1.1 and clip limit equal 0.01 as shown in **Table 48** that the enhancement of quality metrics gave the high values in entropy bilateral or bilateral cascade with nonlocal image filters, sharpness is not enhancement when used nonlocal image filter for wavelet and not enhanced value for CLAHE, SSIM is high value when used bilateral cascade wiener image filters, PSNR is high value for both CLAHE and wavelet when used nonlocal image filter, contrast is not enhancement in CLAHE and it was enhancement in wavelet when used Bilateral or bilateral cascade nonlocal filter image, and low value in noise variance in CLAHE when used bilateral cascade wiener filter and in wavelet when used wiener image filter.

Table 47. Summary quality metrics compared with and without filters used, CLAHE and wavelet transform for a medical normal image.

Medical normal image	Without filters		With Bilateral filter		With wiener image filter		With nonlocal image filter		With Bilateral cascade nonlocal image filters		With Bilateral cascade wiener image filters	
	CLAHE	Wavelet	CLAHE	Wavelet	CLAHE	Wavelet	CLAHE	Wavelet	CLAHE	Wavelet	CLAHE	Wavelet
Entropy	7.5692	5.4941	7.5614	4.2071	7.5644	4.7312	7.5702	5.4961	7.5613	4.2014	7.5611	4.0354
SSIM	0.8032	0.8202	0.8919	0.8813	0.8389	0.8346	0.8077	0.8218	0.8920	0.8813	0.8930	0.8819
PSNR dB	16.6521	16.7133	17.4546	17.1064	16.7943	16.7298	16.6884	16.7838	17.4553	17.1068	17.4681	17.1072
Contrast	0.1837	0.1167	0.1839	0.1204	0.1831	0.1166	0.1839	0.1177	0.1839	0.1204	0.1840	0.1204
Sharpness	0.1320	0.0509	0.0367	0.0143	0.0911	0.0314	0.1248	0.0465	0.0366	0.0142	0.0354	0.0133
Noise variance	0.033729	0.013609	0.033816	0.014504	0.033508	0.013604	0.033834	0.013855	0.033813	0.014505	0.033839	0.014507

Table 48. Summary quality metrics compared with and without filters used CLAHE and wavelet transform for medical pneumonia image.

Medical pneumonia image	Without filters		With Bilateral filter		With wiener image filter		With nonlocal image filter		With Bilateral cascade nonlocal image filters		With Bilateral cascade wiener image filters	
	CLAHE	Wavelet	CLAHE	Wavelet	CLAHE	Wavelet	CLAHE	Wavelet	CLAHE	Wavelet	CLAHE	Wavelet
Entropy	7.4083	5.7206	7.3604	5.1061	7.3945	5.2568	7.4071	5.7215	7.3582	5.0888	7.3560	4.9137
SSIM	0.8443	0.8997	0.9421	0.9437	0.8855	0.9156	0.8446	0.8998	0.9420	0.9436	0.9433	0.9447
PSNR dB	20.1553	21.0716	21.1589	20.5034	20.4197	20.0535	20.1762	21.1009	21.1583	20.4974	21.1388	20.6065
Contrast	0.1673	0.1100	0.1627	0.1174	0.1664	0.1095	0.1673	0.1102	0.1626	0.1174	0.1626	0.1167
Sharpness	0.1725	0.0758	0.0468	0.0266	0.1166	0.0531	0.1721	0.0756	0.0468	0.0266	0.0438	0.0247
Noise variance	0.027999	0.012104	0.026460	0.013790	0.027689	0.011987	0.028004	0.012154	0.026447	0.013782	0.026434	0.013613

4. CONCLUSION

This research has proposed a hybrid enhancement framework of chest X-ray (CXR) images using CLAHE, Haar Wavelet Transform, and some denoising filters such as Bilateral, Wiener,

and Nonlocal Means (NLM) filter. The proposed framework was developed to overcome the common challenges encountered in chest X-ray images, such as low contrast, noise, and low visibility of fine anatomical details. Enhancement was concentrated on tuning two important parameters: adaptive CLAHE clip limit for local contrast enhancement and adaptive Haar wavelet K-factor for edge preservation and enhancement with or without filters. The proposed framework was quantitatively tested by using objective image quality measures, such as PSNR, Structural Similarity Index Measure (SSIM), entropy, contrast, sharpness, and Noise Variance. The experiments showed that the adaptive combination of CLAHE and Haar wavelet achieved remarkable results in enhancing the contrast and structure of images compared to conventional image enhancement techniques. Moreover, using denoising filters efficiently removed noise from the image and improved the quality of image metrics, and retained the important features. The nonlocal means (NLM) filter had the best trade-offs between noise suppression and detail preservation among the filters examined, and the cascade bilateral and Wiener filters had a noticeable improvement across different imaging conditions, for normal image increased the metric SSIM by 11.18% when using CLAHE algorithm, 7.52% when using the wavelet transform, and increased the PSNR by 4.86 % (0.81 dB), 2.37% (0.3972 dB) when using CLAHE, wavelet transform respectively. For medical pneumonia image the cascade Bilateral and Wiener filters gave better values also in SSIM by increasing 11.72%, 5% when using CLAHE, wavelet transform respectively. The PSNR increased by 4.98% (1dB), 0.14% (0.029 dB) when using CLAHE, wavelet transform respectively with Bilateral and Non-Local Means (NLM) filters alone. In conclusion, the proposed framework is an effective preprocessing technique for enhancing chest X-ray images.

Credit Authorship Contribution Statement

Mohanad Azeez Joodi: Writing – review & editing, Writing – original draft, Validation, Software, Methodology. Jaafar Ahmed Abdulsahib: Writing – review & editing, , Software.

Declaration of Competing Interest

The authors declare that they have no known competing financial interests or personal relationships that could have appeared to influence the work reported in this paper.

REFERENCES

Agotra, G., and Singhal, M.K., 2024. A review of image denoising using fuzzy and Wiener filters in the wavelet domain. *International Journal of Scientific Research in Science and Technology*, 11(5), pp. 143-149. https://doi.org/10.32628/IJSRST2411430

Ali, A.A., and Dawood, F.A.A., 2023. Deep learning of diabetic retinopathy classification in fundus images. *Journal of Engineering*, 29(12), pp. 139-152. https://doi.org/10.31026/j.eng.2023.12.09

Anand, S., Roshan, R.K., and Deiveega, S.M., 2023. Chest X ray image enhancement using deep contrast diffusion learning. *Optik*, 279, P. 170751. https://doi.org/10.1016/j.ijleo.2023.170751

Benhassine, N.E., Boukaache, A., and Boudjehem, D., 2021. Medical image denoising using optimal thresholding of wavelet coefficients with selection of the best decomposition level and mother wavelet. *International Journal of Imaging Systems and Technology*, 31(4), pp. 1906-1920. https://doi.org/10.1002/ima.22589

Bian, W., and Yang, Y., 2023. Fast bilateral weighted least square for the detail enhancement of COVID-19 chest X-rays. *Digital Health*, 9, P. 20552076231200981. https://doi.org/10.1177/20552076231200981

Buades, A., Coll, B., and Morel, J.-M., 2005. A non-local algorithm for image denoising. *In Proceedings of the 2005 IEEE Computer Society Conference on Computer Vision and Pattern Recognition (CVPR'05)*, pp. 60-65. https://doi.org/10.1109/CVPR.2005.38

Gamara, R.P.C., Loresco, P.J.M., and Bandala, A.A., 2022. Medical chest X-ray image enhancement based on CLAHE and Wiener filter for deep learning data preprocessing. *In Proceedings of the 2022 IEEE 14th International Conference on Humanoid, Nanotechnology, Information Technology, Communication and Control, Environment, and Management (HNICEM),* pp. 1-6. https://doi.org/10.1109/HNICEM57413.2022.10109585

Ghadi, N.M., and Salman, N.H., 2022. Deep learning-based segmentation and classification techniques for brain tumor MRI: A review. *Journal of Engineering*, 28(12), pp. 93-112. https://doi.org/10.31026/j.eng.2022.12.07

Gonzalez, R.C., and Woods, R.E., 2018. *Digital Image Processing*. Pearson Education, London.

Göreke, V., 2023. A novel method based on Wiener filter for denoising Poisson noise from medical X-Ray images. *Biomedical Signal Processing and Control*, 79, P. 104031. https://doi.org/10.1016/j.bspc.2022.104031

Hentosh, L., Vyklyuk, Y., and Berezsky, O., 2026. Hybrid CUDA acceleration of wavelet-based MRI image denoising. *Frontiers in Signal Processing*, 6, P. 1862897. https://doi.org/10.3389/frsip.2026.1862897

Ismael, A.A., and Baykara, M., 2022. Image denoising based on implementing threshold techniques in multi-resolution Wavelet domain and spatial domain filters. *Traitement du Signal*, 39(4), pp. 1119-1131. https://doi.org/10.18280/ts.390404

Koonsanit, K., Thongvigitmanee, S., Pongnapang, N., and Thajchayapong, P., 2017. Image enhancement on digital X-ray images using N-CLAHE. *In Proceedings of the 2017 10th Biomedical Engineering International Conference (BMEiCON)*, pp. 1-4. https://doi.org/10.1109/BMEiCON.2017.8229130

Liu, X., and Nguyen, T., 2024. Medical images enhancement by integrating CLAHE with wavelet transform and non-local means denoising. *Academic Journal of Computing & Information Science*, 7(1), pp. 52-58. https://doi.org/10.25236/AJCIS.2024.070108

Maruyama, S., 2023. Properties of the SSIM metric in medical image assessment: Correspondence between measurements and the spatial frequency spectrum. *Physical and Engineering Sciences in Medicine*, 46(3), pp. 1131-1141. https://doi.org/10.1007/s13246-023-01280-1

Mooney, P., 2018. *Chest X-Ray Images (Pneumonia)*.

Nayak, T.K., Annavarappu, C.S.R., Nayak, S.R., and Gedefaw, B.M., 2023. DMF-Net: A deep multi-level semantic fusion network for high-resolution chest CT and X-ray image de-noising. *BMC Medical Imaging*, 23, P. 150. https://doi.org/10.1186/s12880-023-01108-0

Nayyef, R.H., and Al-Tammi, M.S.H., 2023. Skull stripping based on the segmentation models. *Journal of Engineering*, 29(10), pp. 74-89. https://doi.org/10.31026/j.eng.2023.10.05

Nia, S.N., and Shih, F.Y., 2024. Medical X-ray image enhancement using global contrast-limited adaptive histogram equalization. *International Journal of Pattern Recognition and Artificial Intelligence*, 38(12), P. 2457010. https://doi.org/10.1142/S0218001424570106

Park, J.-K., Kang, S.-H., Park, M., Lee, D.-H., Kim, K., and Lee, Y., 2022. Noise level and similarity evaluations of non-local means algorithm in chest digital tomosynthesis X-ray imaging system: An experimental study. *Nuclear Instruments and Methods in Physics Research Section A*, 1029, P. 166404. https://doi.org/10.1016/j.nima.2022.166404

Pizer, S.M., Amburn, E.P., Austin, J.D., Cromartie, R., Geselowitz, A., Greer, T., ter Haar Romeny, B.M., Zimmerman, J.B., and Zuiderveld, K.J., 1987. Adaptive histogram equalization and its variations. *Computer Vision, Graphics, and Image Processing*, 39(3), pp. 355-368. https://doi.org/10.1016/S0734-189X(87)80186-X

Pratt, W.K., 2007. *Digital Image Processing: PIKS Scientific Inside*. John Wiley & Sons, Inc., Hoboken. https://doi.org/10.1002/0470097434

Prince, R., Niu, Z., Khan, Z.Y., Emmanuel, M., and Patrick, N., 2024. COVID-19 detection from chest X-ray images using CLAHE-YCrCb, LBP, and machine learning algorithms. *BMC Bioinformatics*, 25, P. 28. https://doi.org/10.1186/s12859-023-05427-5

Priya, M.S., and Rani, M.M.S., 2026. A robust hybrid preprocessing framework integrating DAE, BM3D, median filtering, and CLAHE for enhanced pneumonia chest X-Ray analysis. *International Research Journal on Advanced Science Hub*, 8(5), pp. 199-212. https://doi.org/10.47392/IRJASH.2026.021

Rabbouch, H., Saâdaoui, F., Ibrahim, H., and Zrigui, M., 2022. Multiresolutional hybrid NLM-Wiener filters for X-Ray image denoising. *In Proceedings of the 2022 8th International Conference on Control, Decision and Information Technologies (CoDIT)*, pp. 343-348. https://doi.org/10.1109/CoDIT55151.2022.9804037

Ramos-Soto, O., Ramos-Frutos, J., Rodríguez-Esparza, E., Oliva, D., Pérez-Zarate, E., Carrasco-Hernández, F., and Balderas-Mata, S.E., 2026. Visual enhancement of chest X-ray scans through metaheuristic-based optimization of Gamma correction and CLAHE. *Biomedical Signal Processing and Control*, 113, P. 109153. https://doi.org/10.1016/j.bspc.2025.109153

Rifa'i, A.M., Raharjo, S., Utami, E., and Ariatmanto, D., 2024. Analysis for diagnosis of pneumonia symptoms using chest X-ray based on MobileNetV2 models with image enhancement using white balance and contrast limited adaptive histogram equalization (CLAHE). *Biomedical Signal Processing and Control*, 90, P. 105857. https://doi.org/10.1016/j.bspc.2023.105857

Siracusano, G., La Corte, A., Nucera, A.G., Gaeta, M., Chiappini, M., and Finocchio, G., 2023. Effective processing pipeline PACE 2.0 for enhancing chest X-ray contrast and diagnostic interpretability. *Scientific Reports*, 13, P. 22471. https://doi.org/10.1038/s41598-023-49534-y

Song, J., and Ye, J.C., 2023. Wavelet subband discriminator for efficient unsupervised chest X-ray image restoration. *Medical Physics*, 50(4), pp. 2263-2278. https://doi.org/10.1002/mp.16088

Thamilarasi, V., Asaithambi, A., and Roselin, R., 2025. Enhanced Ensemble Segmentation of Lung Chest X-Ray Images by Denoising Autoencoder and CLAHE. *ICTACT Journal on Image and Video Processing*, 15(3), pp. 3501-3508. https://doi.org/10.21917/ijivp.2025.0496

Thanh, D.N.H., Kalavathi, P., Thanh, L.T., and Prasath, V.B.S., 2020. Chest X-Ray image denoising using Nesterov optimization method with total variation regularization. *Procedia Computer Science*, 171, pp. 1961-1969. https://doi.org/10.1016/j.procs.2020.04.210

Tomasi, C., and Manduchi, R., 1998. Bilateral filtering for gray and color images. *In Proceedings of the Sixth International Conference on Computer Vision,* pp. 839-846. https://doi.org/10.1109/ICCV.1998.710815

Ullah, B., Khan, A., Shah, S.K., Su'ud, M.M., Alam, M.M., and Alam, M., 2023. A Novel Hybrid Framework to Enhance Dual-Energy X-Ray Images. *Journal of Sensors*, 2023, P. 8552175. https://doi.org/10.1155/2023/8552175

Veena, P.V., Devi, G.R., Sowmya, V., and Soman, K.P., 2016. Least square based image denoising using Wavelet filters. *Indian Journal of Science and Technology*, 9(30), pp. 1-6. https://doi.org/10.17485/ijst/2016/v9i30/99023

Wang, Z., Bovik, A.C., Sheikh, H.R., and Simoncelli, E.P., 2004. Image quality assessment: from error visibility to structural similarity. *IEEE Transactions on Image Processing*, 13(4), pp. 600-612. https://doi.org/10.1109/TIP.2003.819861

Zuiderveld, K.J., 1994. *Contrast Limited Adaptive Histogram Equalization*. In Heckbert, P.S. (Ed.), Graphics Gems IV, *Academic Press*, pp. 474-485. https://doi.org/10.1016/B978-0-12-336156-1.50061-6

إطار عمل مختلط لتعزيز صور الأشعة السينية للصدر باستخدام CLAHE و Haar Wavelet ومرشحات تقليل الضوضاء: تحليل مقاييس الجودة

مهند عزيز جودي*، جعفر احمد عبد الصاحب

قسم الهندسة الكهربائية، كلية الهندسة، جامعة بغداد، بغداد، العراق

الخلاصة

يعد التصوير الشعاعي للصدر أحد تقنيات التشخيص الأكثر استخدامًا في التحقيق التشخيصي للأمراض. تقترح هذه الدراسة تقنية تحسين الصورة الهجينة التي تجمع بين معادلة الرسم البياني التكيفي المحدود التباين (CLAHE) مع تحويل مويجات Haar ، بدون استخدام المرشحات, ومع استخدام مرشحات مختلفة لإزالة الضوضاء لتحسين صور الأشعة السينية للصدر. لتحقيق تباين محلي أفضل مع الحفاظ على الحواف، يتضمن الإطار حد مقطع تكيفي في خوارزمية CLAHE وعامل K تكيفي يُستخدم لتحسين تفاصيل شكل موجة Haar. اضافة الى ذلك، تم استخدام مرشحات تقليل الضوضاء الثنائية، ومرشحات Wiener، ومرشحات المتوسط غير المحلي (NLM)، ومرشحات الضوضاء المتتالية لإزالة ضوضاء الصورة مع الحفاظ على المعلومات الهيكلية المهمة. تم استخدام صور الأشعة السينية النموذجية للصدر، سواء في الحالات الطبيعية أو حالات الالتهاب الرئوي، لتقييم طرق التحسين المقترحة. تم استخدام مقاييس موضوعية مثل ذروة نسبة الإشارة إلى الضوضاء (PSNR)، ومؤشر التشابه الهيكلي (SSIM)، والإنتروبيا، والتباين، والحدة، وتباين الضوضاء لقياس جودة الصورة. تشير النتائج التجريبية إلى أن التعديل التكيفي لحد مقطع CLAHE ومؤشر K Haar wave يعزز بشكل كبير جودة الصور مقارنة بالتحسين التقليدي. علاوة على ذلك، فإن تطبيق المرشحات المناسبة لتقليل الضوضاء يمكن أن يحافظ على الهيكل ويقلل من تضخيم الضوضاء دون التضحية بالمعلومات التشخيصية والاستفادة من جميع مقاييس الجودة، خاصة مع المرشح الثنائي المتتالي مع مرشح Wiener والمرشح الثنائي والمرشح غير المحلي وحده. تظهر نتائج التحليل المقارن أن الإطار الهجين المقترح يتفوق دائمًا على الآخرين من حيث مقاييس الجودة المختلفة، مما يؤدي إلى تحسين تصور هياكل الرئة.

الكلمات المفتاحية: مرشح ثنائي، مرشح المتوسط غير المحلي (NLM)، نسبة الإشارة إلى الضوضاء القصوى (PSNR)، مؤشر التشابه الهيكلي (SSIM)، مرشح وينر.